Composite Structures 160 (2017) 8–15

Contents lists available at ScienceDirect

Composite Structures

journal homepage: www.elsevier.com/locate/compstruct

Effect of damage on failure mode of multi-bolt composite joints using failure envelope method

Xiaoquan Cheng [a,*], Songwei Wang [a], Jie Zhang [a], Wenjun Huang [b], Yujia Cheng [a], Jikui Zhang [a,*]

[a] School of Aeronautic Science and Engineering, Beihang University, Beijing 100191, China
[b] AVIC China Helicopter Research and Development Institute, 333001 Jingdezhen, China

ARTICLE INFO

Article history:
Received 24 July 2016
Revised 22 September 2016
Accepted 15 October 2016
Available online 17 October 2016

Keywords:
Damage
Failure mode
Multi-bolt joints
Finite element analysis

ABSTRACT

Failure envelope method is comprehensively used in failure mode prediction of multi-bolt composite joints. The method is based on the assumption that bolt load distribution proportion is constant till failure. However, bearing damage and net-section damage must have some influence on the load distribution and then change structure failure mode. In this paper, tensile experiments of two-bolt and three-bolt joints were conducted to obtain the failure modes and other properties. Three dimensional (3D) finite element models involving damage were constructed, and the results were consistent with experimental data. Then, the models were used to study the effect of damage on failure mode of multi-bolt composite joints. The results show that failure mode prediction with failure envelope method should involve the effect of composite damage. Compared with net-section damage, bearing damage has greater influence on failure mode. Based on conventional failure envelope method, a new evaluation procedure involving damage was proposed.

1. Introduction

Composite materials have been extensively used in aerospace and many other industries. Due to limitations of manufacture and maintenance, bolted joints are quite commonly used in composite structures [1]. However, the drilling of holes cuts the fiber and causes local stress concentration, resulting in reduction of load carrying capacity. To ensure safety and increase weight saving efficiency, the joint structures must be designed seriously, and their mechanical behavior should be studied carefully [2–5]. The failure mode and strength are important properties for composite bolted joints.

The main failure modes of multi-bolt joints include net-section failure, bearing failure and shear out failure as shown in Fig. 1. The bearing failure is a progressive process, while net-section failure and shear out failure occur immediately and catastrophically. The latter two failure modes may reduce the load carrying capacity or cause instant failure of the whole structure. That is the reason why bearing failure mode is preferred in joint structural design and the other two modes should be avoided. By adjusting ±45° layer ratio and the end distance of connected objects, shear out failure can be suppressed and the main failure modes are the other two failure modes. The control of failure modes is very important for bolted joint structure design, thus failure mode prediction methods of multi-bolt composite joints are needed to be investigated.

Many researchers have investigated mechanical properties of single-bolt composite joints [6–8]. Compared with single-bolt joints, there are various load transferring paths in multi-bolt structures, causing more complicated structural characters. Current mechanical investigations on multi-bolt joints mainly focus on bolt load distribution [9–14] and predictions of failure modes and strength. The failure envelope method is a common accepted engineering method for failure mode and failure load prediction.

The failure envelope method is originally proposed by Hart-Smith [15] to predict tensile and bearing failure of double-lap multi-bolt joints with quasi-isotropic or near-quasi isotropic layups. He found that a linear interaction exists between the bearing stress along the bolt hole and the remaining tension stress running by that hole to be reacted elsewhere (bypass stress). Based on the experimental results, he proposed the bearing-bypass failure envelope. Then, Crews and Naik [16], Rao et al. [17], Camanho et al. [18,19], Bois et al. [20] applied and developed the method. In the failure envelope, the line corresponding to bearing failure is a contour line determined by single-bolt bearing strength. But Liu et al.

* Corresponding authors.
E-mail addresses: xiaoquan_cheng@buaa.edu.cn (X. Cheng), zjk@buaa.edu.cn (J. Zhang).

http://dx.doi.org/10.1016/j.compstruct.2016.10.042
0263-8223/

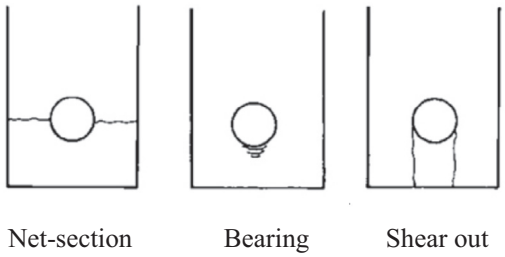

Fig. 1. Failure modes of multi-bolt composite joints.

[10,21] indicated that bypass load influences bearing failure strength, and corrected the failure envelope.

But all these researchers assumed that bearing stress and bypass stress has a constant ratio throughout the failure process. As a matter of fact, load distribution between bolts would change once composite damage occurs, and the bearing and bypass stress ratios can also be affected. Therefore, the effect of damage on failure mode of multi-bolt composite joints using the failure envelope method deserves to be further explored.

In the present paper, theory of failure envelope method was briefly introduced. Tensile experiments of two-bolt and three-bolt composite joints were conducted, and 3D finite element models considering damage were constructed. Based on the numerical model, bolt load distribution was investigated, and the effect of composite damage on failure mode was analyzed.

2. Theory of failure envelope method

Principle of the failure envelope method is shown in Fig. 2. Line ACE is the failure envelope of multi-bolt composite joints, and it can be obtained by single-bolt joint bearing experiment and open-hole laminate tensile experiment.

Line AC represents the cut-off line of ultimate bearing failure and line CE represents that of ultimate net-section failure. The failure envelope is related with joint geometry and laminate stacking sequence, et al.

Bearing stress at point A corresponds to the ultimate bearing failure strength of single-bolt laminates σ_{bru}, Bypass stress at point E is related to ultimate net-section tensile failure strength of open-hole laminates σ_{netu}.

The strength equations are shown as following:

$$\sigma_{bru} = F_{bru}/Dt \tag{1}$$

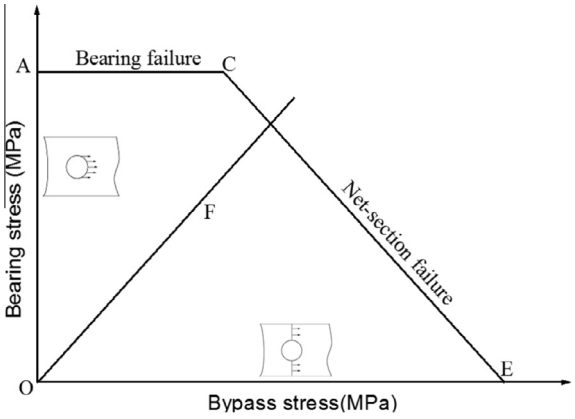

Fig. 2. Sketch map of failure envelope method.

$$\sigma_{netu} = F_{netu}/(W - D)t \tag{2}$$

where F_{bru} and F_{netu} denote bearing and net-section tensile failure loads respectively. D denotes hole diameter, t denote laminate thickness, and W denotes laminate width. Equation of line CE is

$$K_{brc}\sigma_{br} + K_{tc}\sigma_{by} = \sigma_t \tag{3}$$

where K_{brc} denotes the stress concentration factor caused by loaded-hole tensile stress, while K_{tc} denotes the stress concentration factor caused by open-hole tensile stress. σ_{br} and σ_{by} denotes bearing and bypass stresses respectively. σ_t denotes the laminate tensile strength.

The two factors could be calculated by the composite stress concentration relief factor C_{re} from elastic isotropic stress concentration factors K_{te} (net-section tension) and K_{bre} (bearing stress), respectively.

$$K_{brc} = 1 + C_{re}(K_{bre} - 1) \tag{4}$$

$$K_{tc} = 1 + C_{re}(K_{te} - 1) \tag{5}$$

Bearing and bypass stresses show linear relationship under applied load and that is described by line OF. The slope of line OF is shown as following:

$$K = \sigma_{br}/\sigma_{by} \tag{6}$$

in which,

$$\sigma_{by} = F_{by}/(W - D)t \tag{7}$$

$$\sigma_{br} = F_{br}/Dt \tag{8}$$

where F_{by} and F_{br} are the bypass and bearing loads, respectively. Bypass stress σ_{by} and bearing stress σ_{br} increase with the applied load, resulting in growth of line OF. When line OF intersects with failure envelope, the joint gets ultimate failure. Bearing failure occurs with the intersection at line AC, while net-section failure occurs with the intersection at line CE.

As mentioned before, the method is based on the hypothesis that joint failure is a linear process with constant load distribution. This simplifies the analysis but loses important information such as damage. In application of composite joints, the damage is likely to occur before their ultimate failure. When damage occurs in multi-bolt joint, the load distribution will change with the variation of K, and this may vary the failure mode.

3. Methodology

3.1. Specimen and experimental procedures

The experiment included two specimen groups: two-bolt joint (J2) and three-bolt joint (J3). There were three specimens in J2 group and two specimens in J3 group. The two groups had the same material and joint parameters except bolt number. Geometry of J3 is shown schematically in Fig. 3. For convenience of reference, bolts and holes are numbered 1# to 3# from left to right.

The fixture and specimens were made from carbon/epoxy composite materials T300/5228A. Laminates had a quasi-isotropic stacking sequence of $[0/45/90/-45]_{3S}$. The mechanical properties of the composite material are listed in Table 1[22]. The bolts with diameter of 6 mm were made from aerospace grade Titanium alloy, whose modulus and Poisson's ratio are 110 GPa and 0.3, respectively. Washers were placed on both sides of the laminate.

Specimens were assembled with bolt torque of 0.5Nm. The torque could represent the worst assembly condition of joint. On the other hand, it could reduce friction between specimen and fixtures to make the load transferring through bolts.

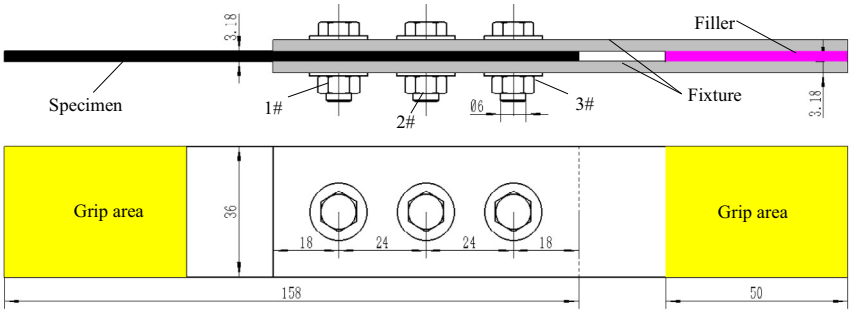

Fig. 3. Geometry of three-bolt joint.

Table 1
Mechanical properties of T300/5228A [22].

Elastic property	Value	Strength property	Value
E_{11} (GPa)	144	X_t (MPa)	1633
E_{22} (GPa)	9.31	X_c (MPa)	1021
E_{33} (GPa)	9.31	Y_t (MPa)	53.8
G_{12} (GPa)	4.68	Y_c (MPa)	212
G_{12} (GPa)	3.00	S_{12} (MPa)	80.4
G_{12} (GPa)	4.68	S_{23} (MPa)	103
$\nu_{12},\nu_{23},\nu_{13}$	0.31	S_{13} (MPa)	103

The experiments were conducted in INSTRON 8801 test machine at room temperature. Specimens were loaded with displacement rate of 1 mm/min. J2 group has the same procedure as J3 group.

To obtain the failure envelope of ACE, open-hole tensile and single-bolt bearing experiments were conducted. The specimens were manufactured with the same batch of material. Geometry and experimental procedures referred to the ASTM with three specimens in each group.

3.2. Numerical model

Due to the difficulty of detecting damage around holes and testing load distribution by experiment, finite element (FE) method is required. The numerical model were constructed using commercial software Abaqus/Standard [23].

The joints were modeled by eight-node C3D8R brick elements. Considering the unsymmetry of off-axis plies, the joint was not simplified by half model. All composite laminates were modeled by "composite layup" with each layup containing four layers in the thickness direction. The meshes were refined around the hole where the stress concentration is severe. 40 elements were meshed around each laminate hole. The mesh of J3 is shown in Fig. 4. One end of the joint was fixed and the other was applied x-direction tensile displacement load. Since the bolt torque was small enough in the experiment, bolt preload was ignored. In order to simulate the contact condition, surface to surface contact pairs were constructed. The contact property was defined as "hard" contact in the normal direction to transfer enough pressure between contact surfaces. In the tangential direction, the "penalty" model was chosen with friction coefficient of 0.2 between contact surfaces. The contact property was applied to the lamina-to-lamina and lamina-to-bolt contacts. According to the guideline of the software, the bolts were chosen the master surface for the lamina-to-bolt contact, and the middle plate was the master surface for the lamina-to-lamina contact.

In order to simulate the composite damage and failure process, composite failure criteria and degradation rules were used. The widely accepted Hashin-type failure criteria [24–26] were chosen here. The material degradation rules are of great significance in modeling progressive damage behavior of composite materials. Though many researchers have devoted efforts to studying them [27], there are no common accepted degradation rules. Chang [28] predicted net-section tensile failure of open-hole laminate well with degradation rules of related moduli to zero once corresponding failure occurs, and McCarthy [13] predicted bearing failure of bolted laminate with degradation rules of related moduli to specific values once corresponding failure occurs. Therefore, Chang's and McCarthy's degradation rules were adopted for tensile failure (caused by net-section load) and compressive failure (caused by bearing load), respectively. The details of composite failure criteria and degradation rules are shown in Table 2. The progressive damage analysis was conducted based on VUSDFLD code, which can be called in Abaqus to redefine field variables at material points. Fig. 5 shows the schematic diagram of progressive damage analysis process.

4. Results

4.1. Comparison of experimental and numerical results

A comparison of experimental and numerical ultimate loads is listed in Table 3. It can be seen that only small variation exists within the groups, and the numerical results are in agreement with the average values of experimental data.

The experimental and numerical load-displacement curves are shown in Fig. 6. The curves experience two stages before ultimate

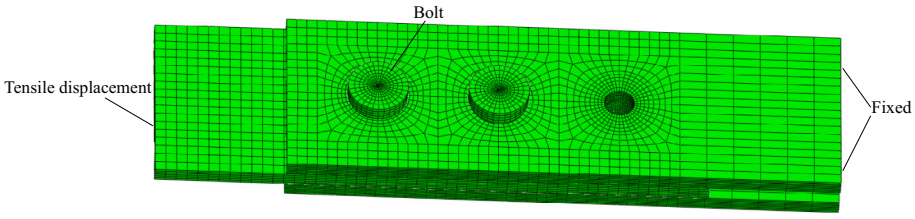

Fig. 4. Meshes and boundary conditions of J3 model.

Table 2
Composite failure criteria and degradation rules.

Failure modes	Failure criteria	Degradation rules
Fiber tensile failure	$\left[\frac{\sigma_1}{X_C}\right]^2 \geqslant 1$	$E_{11} = E_{22} = E_{33} = G_{12} = G_{23} = G_{13} = \mu_{12} = \mu_{13} = \mu_{23} = 0$
Fiber compressive failure	$\left[\frac{\sigma_1}{X_T}\right]^2 + \left[\frac{\tau_{12}}{S_{12}}\right]^2 + \left[\frac{\tau_{13}}{S_{13}}\right]^2 \geqslant 1$	$E_{11} = 0.2E_{11}\ E_{22} = 0.2\ E_{22}E_{33} = 0.2E_{33}\ G_{12} = 0.2\ G_{12}G_{23} = 0.2G_{23}\ G_{13} = 0.2\ G_{13}\mu_{12} = \mu_{13} = \mu_{23} = 0.1\mu_{12}$
Matrix tensile failure	$\left[\frac{\sigma_2}{Y_t}\right]^2 + \left[\frac{\tau_{12}}{S_{12}}\right]^2 + \left[\frac{\tau_{23}}{S_{23}}\right]^2 \geqslant 1$	$E_{22} = \mu_{12} = 0$
Matrix compressive failure	$\left[\frac{\sigma_2}{Y_C}\right]^2 + \left[\frac{\tau_{12}}{S_{12}}\right]^2 + \left[\frac{\tau_{23}}{S_{23}}\right]^2 \geqslant 1$	$E_{22} = 0.2E_{22}\mu_{12} = 0.2\mu_{12}$
Fiber matrix shear failure	$\left[\frac{\sigma_1}{X_C}\right]^2 + \left[\frac{\tau_{12}}{S_{12}}\right]^2 + \left[\frac{\tau_{13}}{S_{13}}\right]^2 \geqslant 1$	$G_{12} = \mu_{12} = 0$
Tensile delamination	$\left[\frac{\sigma_3}{Y_T}\right]^2 + \left[\frac{\tau_{12}}{S_{12}}\right]^2 + \left[\frac{\tau_{13}}{S_{13}}\right]^2 \geqslant 1$	$E_{33} = G_{23} = G_{13} = \mu_{23} = \mu_{13} = 0$
Compressive delamination	$\left[\frac{\sigma_3}{Y_C}\right]^2 + \left[\frac{\tau_{12}}{S_{12}}\right]^2 + \left[\frac{\tau_{13}}{S_{13}}\right]^2 \geqslant 1$	$E_{33} = G_{23} = G_{13} = \mu_{23} = \mu_{13} = 0$

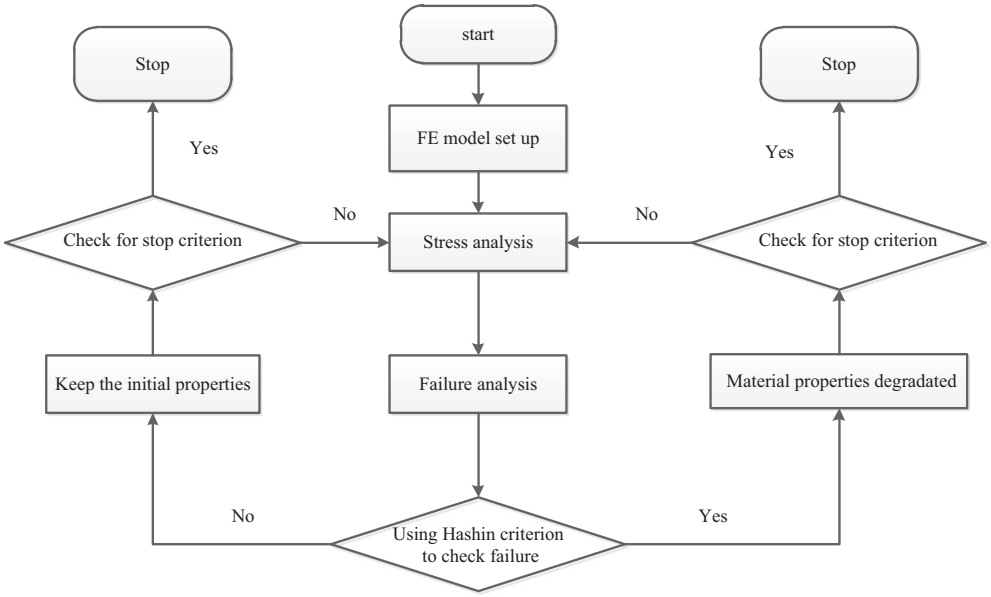

Fig. 5. Schematic diagram of progressive damage analysis process [29].

Table 3
Experimental and numerical ultimate loads.

Joint	Experiment (kN)	Average (kN)	FE (kN)	Error (%)
J2-1	24.4			
J2-2	24.8	24.9	24.8	0.4
J2-3	25.5			
J3-1	25.7	25.75	27.7	7.5
J3-2	25.8			

failure: linear stage and nonlinear stage. Within each group, linear stage of the experimental curves is similar while some variations exist in the nonlinear stage, but the ultimate load is almost the same. The FE model could predict linear stage very well and nonlinear stage in acceptable range.

The failure profiles of J2 and J3 are shown in Figs. 7and 8 respectively. It is observed that experimental results are identical within the group. The failure modes of both J2 and J3 are net-section failure in 1# hole. Besides, other damage could be seen around the holes. Both two holes show obvious bearing damage in J2 group, while the damage is nearly invisible in J3 group. Thus the specimen of J3-1 was cut and detected under microscope. It can be found that 1# and 2# holes present minor bearing damage, while 3# hole is undamaged. The numerical results of J2 and J3 show that damage around 1# hole extends to laminate edge along the width direction with bearing damage around the other holes, which are consistent with experimental results.

Based on the comparison of ultimate loads, load-displacement curves and failure profiles, the numerical model can be used to predict tensile behavior of multi-bolt composite joint. The failure process of J3 predicted by numerical model is as follows: in the linear stage, the stress around 1# hole is the most severe among three holes; then bearing damage initiates from 1# hole in a small region and the load-displacement curve becomes nonlinear. With the load increasing continuously, net-section damage occurs around 1# hole, and bearing damage occurs around 2# hole. Finally, the net-section damage at 1# hole extends to the whole section and causes ultimate failure. The failure process of J2 is basically identical to J3, but bearing damage regions around holes are larger.

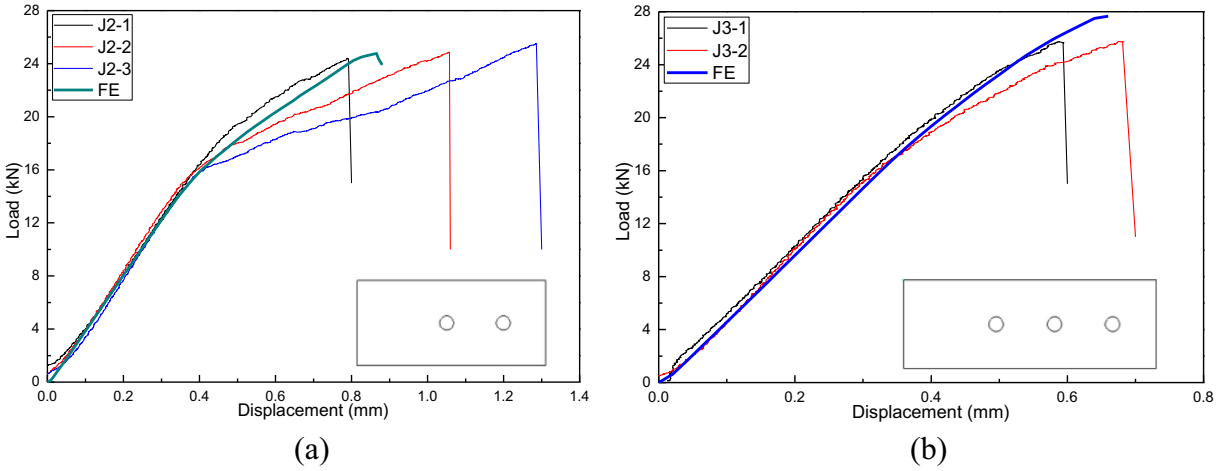

Fig. 6. Experimental and numerical load-displacement curves. (a) J2. (b) J3.

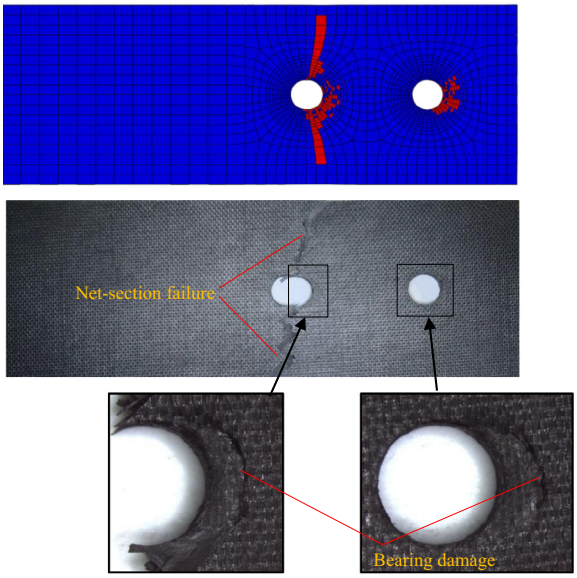

Fig. 7. Failure profiles of J2-1.

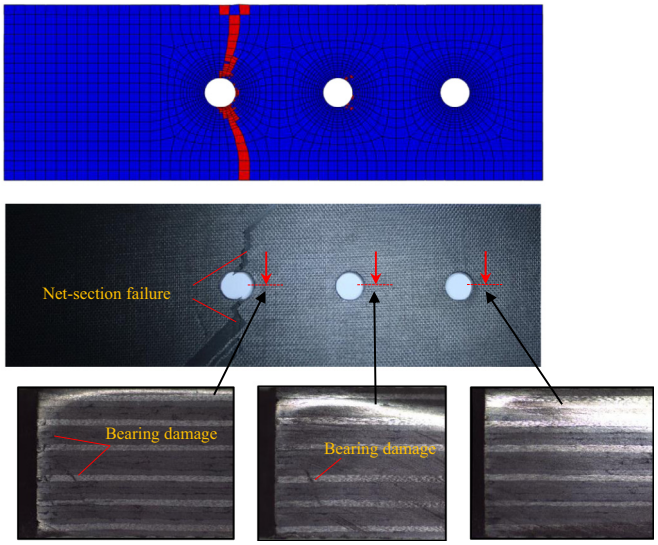

Fig. 8. Failure profiles of J3-1.

4.2. Effect of bearing damage on failure mode

Experimental and numerical results show that initial damage mode of each hole in J2 and J3 is bearing failure. Therefore, the effect of bearing damage was studied firstly.

According to the procedure of failure envelope method, the first step is the calculation of bolt load distribution. Bolt load was obtained by the contact force between bolt and composite laminate hole, and bolt load and their distribution ratio were calculated. Their curves of J2 and J3 are shown in Fig. 9.

Similar to load-displacement curves, the bolt loads of J2 and J3 experience linear and nonlinear stages. In the linear stage, the load distribution ratio is obviously non-uniform but constant. After damage occurs, the curves become nonlinear. The nonuniformity of bolt load reduces and the load distribution ratio changes. From Fig. 9, the bolt load of 1# is much larger than the others in the linear stage but close to the others in the nonlinear stage. 1# load distribution ratio drops from 56% to 52% in J2 and from 44% to 36% in J3. Nevertheless, 1# bolt carries the maximum load in both J2 and J3 during the loading process.

For 1# hole in J3, the bypass load is equal to sum of 2# and 3# bolt load. Similarly, bypass load of 2# hole is equal to the 3# bolt load. 3# hole only has bearing load equal to 3# bolt load. Therefore, 1# hole has the maximum net-section load among the three holes. The case is same for J2.

Since 1# hole carries maximum bearing load and maximum bypass load, it is determined to be the critical location. 1# hole is focused on in failure mode analysis of J2 and J3. The calculated bearing stress vs. bypass stress curves are plotted in failure envelope chart as shown in Fig. 9. OF_i is the bearing stress vs. bypass stress curve of J*i* ($i = 2, 3$). As the load distribution ratio of 1# bolt for J2 is larger than that for J3, OF_2 has a sharper slop than OF_3. Although there are differences between these two curves, their trends are similar. The curves keep linear until damage initiation, and then become gentle as 1# bolt load decreases. The curves intersect with CE and present net-section failure.

As mentioned in section methodology, failure envelop ACE is obtained by experimental tests. Fig. 10 shows tested one bolt bearing strength and open-hole tensile strength as points A and E. According to [30], the stress concentration relief factor is set to be 0.25 and line CE could be calculated.

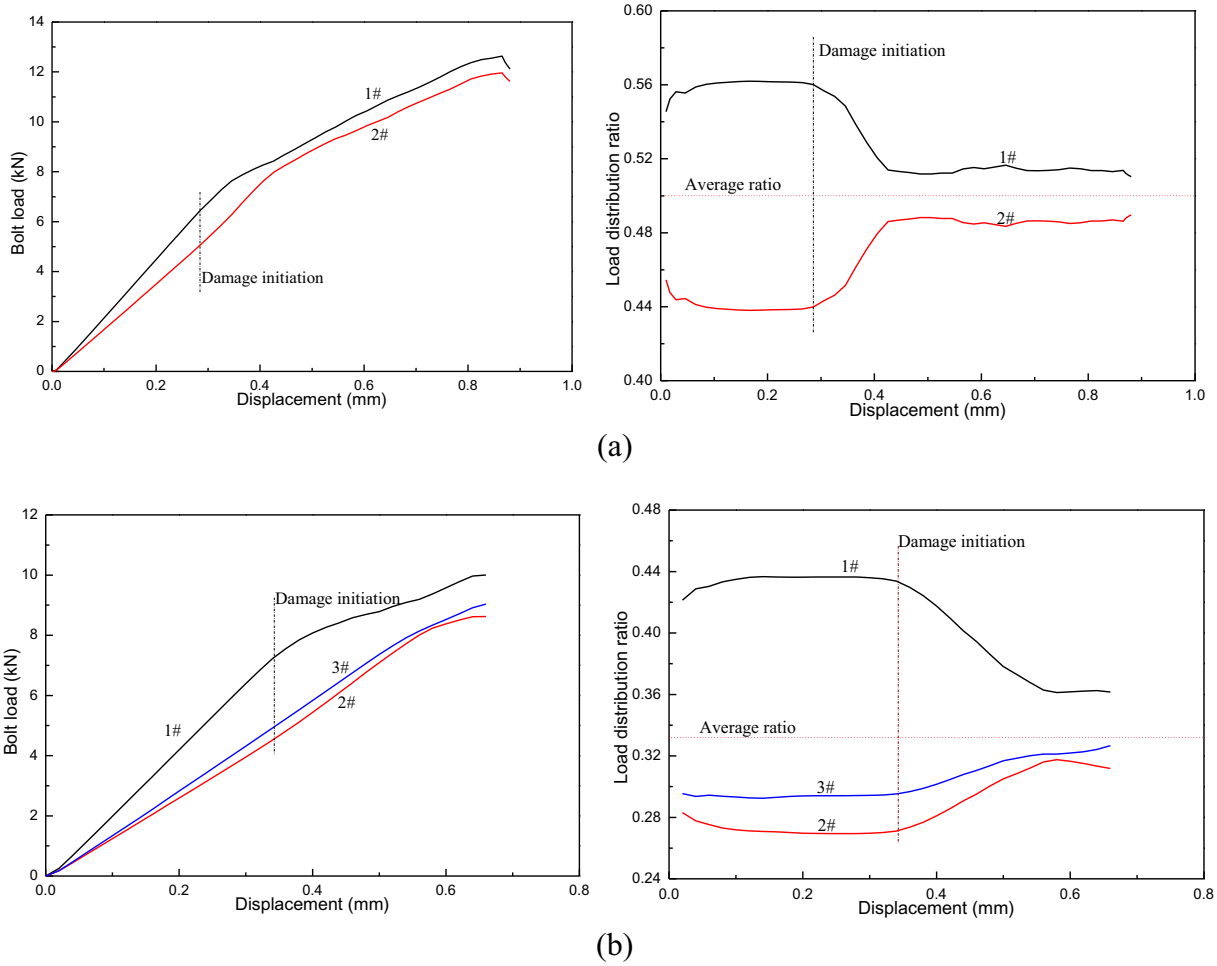

Fig. 9. Bolt load and load distribution ratio curves. (a) J2. (b) J3.

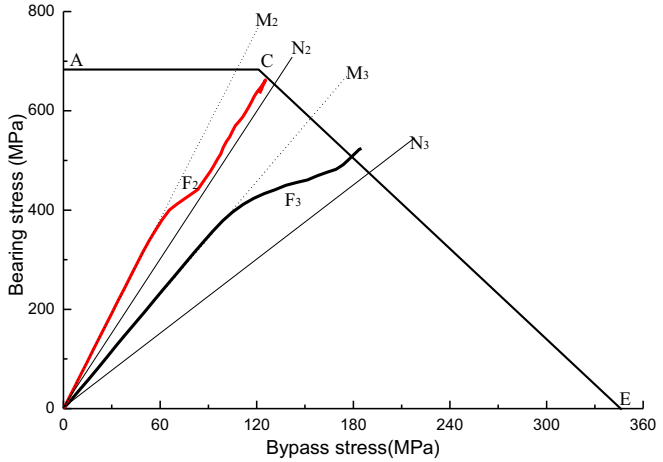

Fig. 10. Bearing stress vs. bypass stress curves of 1# hole in failure envelope chart.

Two additional curves are drawn in Fig. 10. OM_i is the stress curve ignoring composite damage and ON_i is the stress curve supposing that load distributes uniformly in each bolt. It can be noticed that OF and OM coincide before damage initiation. If damage is ignored, OF would have the same slop with OM and the predicted failure mode would be decided by the intersection point of OM and failure envelope. However, the damage changes the tendency of OF. The failure mode prediction of J2 is bearing failure by OM but net-section failure by OF. Compared with experimental results, OF can give right failure mode prediction. Although OM and OF predict the same failure mode for J3, the bearing and bypass stress states are different. This proves that the damage can affect the stress state and even the failure mode. Therefore, the effect of damage is not neglectable. Bearing damage could decrease the slop of OF, some bearing failure of joints may transform to net-section failure. Note that OF varies between OM and ON, the two curves give a range of the failure mode.

In conclusion, the bearing damage could decrease the bearing stress and change the tendency of bearing stress vs. bypass stress curve. The joint load distribution and even the failure mode are influenced.

4.3. Effect of net-section damage on failure mode

In order to get net-section damage, a new model of J3 was constructed, in which the width was changed to 20 mm. The bolt load and load distribution ratio of the new model are shown in Fig. 11.

Nonuniformity of the bolt load distribution is more severe than that of the original model since the load ratio of 1# bolt reached 54%. Furthermore, bolt load and load distribution ratio show a small decrease after damage occurs.

Fig 12 shows the bearing stress vs. bypass stress curve of the new model with net-section damage. The curve has the same tendency with original model that the slop decreases after damage

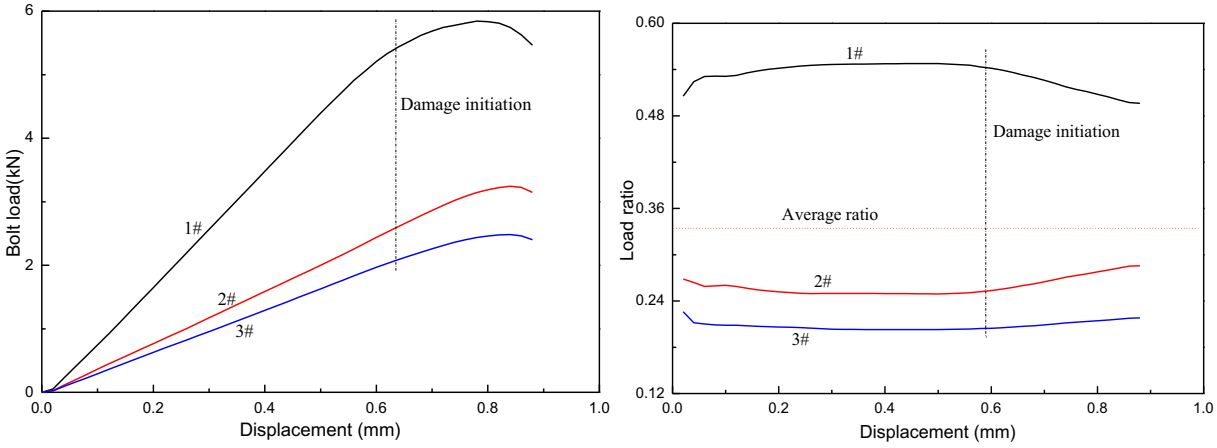

Fig. 11. Bolt load and load distribution ratio of the new J3 model.

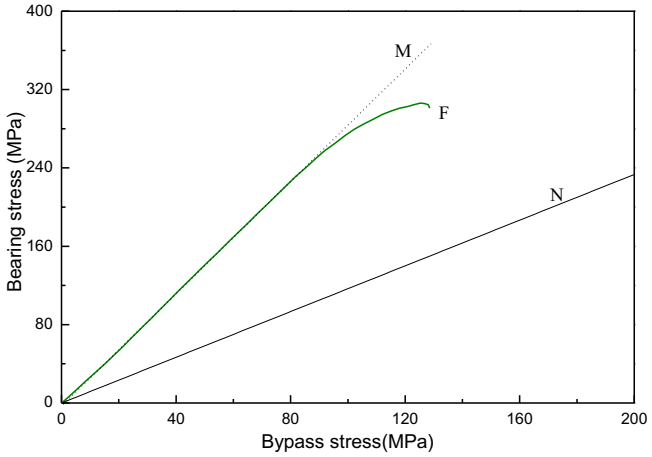

Fig. 12. Bearing stress vs. bypass stress curve of the new J3 model.

initiation. But the decrease is limited and the ultimate failure occurs subsequently. To some extent, net-section damage can also affect the failure mode from bearing failure to net-section failure. It can be seen that OF also varies between OM and ON.

5. Discussion

Results of different models show that bearing or net-section damage occurs before ultimate failure. The two damage modes can both relieve the stress of 1# bolt, hence load distribution changes. The slop of bearing vs. bypass stress curve decreases after damage initiation, and the curve deflects from the original tendency. Some of bearing failure may change to net-section failure. Thus predicting failure mode using failure envelope method must consider the effect of damage, and the method should be improved.

The variation of load distribution caused by bearing damage is larger than that by net-section damage. No matter bearing damage or net-section damage, the stress curve OF is between OM and ON, and the variation range of failure mode can be determined. The procedure for failure mode prediction based on failure envelope method is proposed.

Firstly, calculate the load distribution of the joint structures without damage and draw straight line ON.

Secondly, equalize the load distribution and draw straight line OM.

Thirdly, analyze the intersection of OM and ON with the failure envelope:

If both OM and ON intersect with AC, the ultimate failure mode is bearing failure.

If both OM and ON intersect with CE, the ultimate failure mode is net-section failure.

If OM intersects with AC and ON with CE, the ultimate failure mode is undetermined, and detailed experimental or numerical analysis should be conducted.

6. Conclusions

In this paper the effect of damage on failure mode of multi-bolt composite joint using failure envelope method was studied. Experiments of two-bolt and three-bolt composite joints were conducted, and 3D finite element models containing composite damage were constructed. Bolt load distribution, bearing stress and bypass stress were calculated. Failure mode of the composite joints was predicted, and the effect of bearing damage and net-section damage were analyzed. These conclusions can be obtained:

(1) Bearing damage and net-section damage can relieve the critical hole stress and change bolt load distribution with slope variation of the bearing vs. bypass stress curve. Therefore, composite damage must be considered in failure envelope method.
(2) The failure mode of multi-bolt composite joints may change from bearing failure to net-section failure when damage is considered. The effect of bearing damage is greater than that of net-section damage.
(3) OF (real stress curve) is limited between OM (curve neglecting damage) and line ON (curve supposing load uniformly distributed among bolts). When OM and ON intersect with the same line in failure envelope, structural failure mode can be determined with them. But structural failure mode is uncertain when OM and ON intersect with different lines, and further analysis is required.

References

[1] McCarthy MA, McCarthy CT, Padhi GS. A simple method for determining the effects of bolt–hole clearance on load distribution in single-column multi-bolt composite joints. Compos Struct 2006;73(1):78–87.
[2] Sen F, Sayman O. Experimental failure analysis of two-serial-bolted composite plates. J Appl Polym Sci 2009;113(1):502–15.

[3] Zhou S, Wang Z, Zhou J, et al. Experimental and numerical investigation on bolted composite joint made by vacuum assisted resin injection. Compos Part B Eng 2013;45(1):1620–8.
[4] Ascione F, Feo L, Maceri F. On the pin-bearing failure load of GFRP bolted laminates: an experimental analysis on the influence of bolt diameter. Compos Part B Eng 2010;41(6):482–90.
[5] Wang SW, Cheng XQ, Guo X, et al. Influence of lateral displacement of the grip on single lap composite-to-aluminum bolted joints. Exp Mech 2016;56 (3):407–17.
[6] Hassan NK, Mohamedien MA, Rizkalla SH. Finite element analysis of bolted connections for PFRP composites. Compos Part B Eng 1996;27(3-4):339–49.
[7] Xiao Y, Ishikawa T. Bearing strength and failure behaviour of bolted composite joints (part II: modelling and simulation). Compos Sci Technol 2005;65:1032–43.
[8] Feo L, Marra G, Mosallam AS. Stress analysis of multi-bolted joints for FRP pultruded composite structures. Compos Struct 2012;94(12):3769–80.
[9] Lecomte J, Bois C, Wargnier H, et al. An analytical model for the prediction of load distribution in multi-bolt composite joints including hole-location errors. Compos Struct 2014;117:354–61.
[10] Liu F, Zhang J, Zhao L, et al. An analytical joint stiffness model for load transfer analysis in highly torqued multi-bolt composite joints with clearances. Compos Struct 2015;131:625–36.
[11] Ekh J, Schön J. Load transfer in multirow, single shear, composite-to-aluminium lap joints. Compos Sci Technol 2006;66:875–85.
[12] Taheri-Behrooz F, Kashani ARS, Hefzabad RN. Effects of material nonlinearity on load distribution in multi-bolt composite joints. Compos Struct 2015;125:195–201.
[13] Lawlor VP, McCarthy MA, Stanley WF. An experimental study of bolt–hole clearance effects in double-lap, multi-bolt composite joints. Compos Struct 2005;71:176–90.
[14] McCarthy CT, McCarthy MA, Lawlor VP. Progressive damage analysis of multi-bolt composite joints with variable bolt–hole clearances. Compos Part B Eng 2005;36(4):290–305.
[15] Hart-Smith LJ. Bolted joints in graphite-epoxy composites. NASA CR-144899. Long Beach: Douglas Aircraft Company; 1976.
[16] Crews JH, Naik RA. Combined bearing and bypass loading on a graphite/epoxy laminate. NASA-TM-87705. Hampton: Langley Research Center; 1986.
[17] Rao B, Shankar G, Krishnaraj V, Krishna K. Stress concentration and its effect on composite bolted joints. In: International symposium of research students on materials science and engineering: ISRS-2004. Chennai, India; 2004. p. 1–10.
[18] Camanho PP, Matthews FL. Stress analysis and strength prediction of mechanically fastened joints in FRP-a review. Compos Part A 1997;28:529–47.
[19] Camanho PP, Lambert M. A design methodology for mechanically fastened joints in laminated composite materials. Compos Sci Technol 2006;66:3004–20.
[20] Bois C, Wargnier H, Wahl JC, et al. An analytical model for the strength prediction of hybrid (bolted/bonded) composite joints. Compos Struct 2013;97:252–60.
[21] Liu F, Zhao L, Mehmood S, et al. A modified failure envelope method for failure prediction of multi-bolt composite joints. Compos Sci Technol 2013;83:54–63.
[22] Liu P, Cheng XQ, Wang SW, et al. Numerical analysis of bearing failure in countersunk composite joints using 3D explicit simulation method. Compos Struct 2016;138:30–9.
[23] ABAQUS. Analysis user manual. Version 6.9. Dassault Systèmes; 2010.
[24] Thoppul SD, Finegan J, Gibson RF. Mechanics of mechanically fastened joints in polymer–matrix composite structures–a review. Compos Sci Technol 2009;69 (3):301–29.
[25] Liu PF, Zheng JY. Recent developments on damage modeling and finite element analysis for composite laminates: a review. Mater Des 2010;31(8):3825–34.
[26] Hashin Z. Failure criteria for unidirectional fiber composite. J Appl Mech 1980;47(2):329–34.
[27] Garnich MR, Akula VMK. Review of degradation models for progressive failure analysis of fiber reinforced polymer composites. Appl Mech Rev 2009;62 (1):1–33.
[28] Chang FK, Lessard LB. Damage tolerance of laminated composites containing an open-hole and subjected to compressive loadings. I: analysis. J Compos Mater 1991;25(1):2–43.
[29] Zhang Q, Cheng XQ, Zhang J, et al. Experimental and numerical investigation of composite box joint under tensile load. Compos Part B Eng 2016;107:75–83.
[30] Xie M, Li G, Li W, et al. Joints for composites materials. Shanghai: Shanghai Jiao Tong University Press; 2011.